MEDICAL SCIENCE MONITOR

CLINICAL RESEARCH

e-ISSN 1643-3750
© Med Sci Monit, 2020; 26: e923559
DOI: 10.12659/MSM.923559

Received: 2020.02.17
Accepted: 2020.04.01
Available online: 2020.05.07
Published: 2020.05.14

miR-20a/Foxj2 Axis Mediates Growth and Metastasis of Colorectal Cancer Cells as Identified by Integrated Analysis

Authors' Contribution:
Study Design A
Data Collection B
Statistical Analysis C
Data Interpretation D
Manuscript Preparation E
Literature Search F
Funds Collection G

E 1 Yong Qiang*
B 2 Liang Feng*
C 3 Gang Wang*
B 1 Jian Liu
C 1 Jing Zhang
D 1 Lanlan Xiang
E 1 Chunjie Su
F 1 Songbai Zhang
F 1 Xiongwei Xie
A 4 Erlin Chen

1 Department of General Surgery, Jingmen No. 1 People's Hospital, Jingmen, Hubei, P.R. China
2 Department of Burn and Plastic Surgery, Affiliated Nantong Hospital No. 3 of Nantong University, Nantong, Jiangsu, P.R. China
3 Department of Anesthesiology, Union Hospital Affiliated with Tongji Medical College of Huazhong University of Science and Technology, Wuhan, Hubei, P.R. China
4 Department of General Surgery, Affiliated Hospital of Nantong University, Nantong, Jiangsu, P.R. China

* Yong Qiang, Liang Feng and Gang Wang contributed equally to this work

Corresponding Authors: Erlin Chen, e-mail: calntmu@163.com, Xiongwei Xie, e-mail: xiexiongweigs@aliyun.com
Source of support: This research was funded by a grant from the Jingmen Science and Technology Project (YFYB2016005)

Background: MicroRNAs (miRNAs) have a significant regulatory effect on the proliferation, migration, and invasion of cells, and have been widely reported to have oncogenic or tumor-suppressive impacts on various tumors. In the present study we assessed the regulation and function of miR-20a on colorectal cancer (CRC) cell lines.

Material/Methods: qPCR was used to quantify miR-20a expression. Luciferase reporter assay was conducted to confirm Foxj2 3'UTR associations. In addition, the function of miR-20a and Foxj2 in CRC was detected using MTT, colony formation, transwell assays, and cell cycle analysis.

Results: Our data revealed that miR-20a expression was elevated in the CRC cell lines, and cell migration, proliferation, and invasion abilities were promoted by the overexpression of miR-20a. Moreover, Foxj2 was authenticated as a direct target gene of miR-20a in CRC cells. Furthermore, we found that the ectopic Foxj2 dramatically suppressed miR-20a-promoted proliferation, migration, invasion, and xenografts *in vitro* and *in vivo*, and induced cell cycle arrest at G1 stage.

Conclusions: Our results showing the roles of miR-20a/Foxj2 in carcinogenesis of CRC may help improve treatment of CRC.

MeSH Keywords: Colorectal Neoplasms, Hereditary Nonpolyposis • MicroRNAs • Tumor Markers, Biological

Full-text PDF: https://www.medscimonit.com/abstract/index/idArt/923559

3334 1 5 32

Indexed in: [Current Contents/Clinical Medicine] [SCI Expanded] [ISI Alerting System] [ISI Journals Master List] [Index Medicus/MEDLINE] [EMBASE/Excerpta Medica] [Chemical Abstracts/CAS]

Background

Colorectal cancer (CRC) is a common malignant tumor that is one of the leading causes of cancer-related death worldwide [1]. In developed Western countries, CRC is the second most common cancer, and morbidity and mortality rates are continually increasing in China [2]. The onset of CRC is subtle, early symptoms are mild or inconspicuous; therefore, many patients are diagnosed in the middle and late stages of CRC, with poor response to treatment unfavorable prognosis. The 5-year survival rate of advanced metastatic CRC is less than 10%, and it has the fifth-highest cancer mortality rate in China. Although is increasing understanding, improved diagnosis, and more effective therapy of CRC, the precise molecular mechanisms underlying disease initiation and progression are complicated and ambiguous. Therefore, it is of great clinical significance to identify biomarkers related to CRC.

miRNAs repress gene expression, mainly by direct interaction with the 3'-untranslated regions (3'UTRs) of mRNAs, and belong to a cluster of highly conserved, small, non-coding RNAs [3]. miRNAs can serve as either tumor oncogenes or inhibitors, and take part in many biological processes, including cell proliferation, differentiation, and apoptosis, by targeting various transcripts, and are associated with the initiation, promotion, and development of all types of human cancer [4]. With the development of molecular genetics, growing evidence proved that miR-20a is expressed at higher levels in CRC tissues than in normal adjacent mucosal tissues, and patients with elevated expression levels of miR-20a have larger lymph nodes. The high incidence of distant metastasis suggests that miR-20a can regulate the metastasis of CRC. Li et al. indicated that the level of miR-20a was considerably higher in CRC tissues and is correlated with the apoptosis and distant metastasis of cancer cells. Additionally, miR-20a plays a role in migration, invasion, and epithelial-to-mesenchymal transition (EMT) of CRC cells by regulating the underexpression E-cadherin and overexpression of vimentin. However, the mechanism through which miR-20a affects the development of CRC is unclear.

In the present work, integrated analyses were performed and miR-20a was screened as an oncogenic molecule in CRC, suggesting that the level of miR-20a was upregulated in CRC cells and tissues. The overexpressed miR-20a positively regulated cell proliferation and colony formation. Additionally, Foxj2 was identified as a hub target of miR-20a based on the integrated bioinformatics analysis and *in vitro* experiments. Subsequently, the regulation of miR-20a on Foxj2 was also verified, showing that cell migration and invasion were promoted by miR-20a by suppressing the expression of Foxj2.

Material and Methods

Integrated analysis of CRC miRNA and mRNA datasets

The gene and miRNA expression data and the relevant clinical information of TCGA-COAD were extracted from The Cancer Genome Atlas (TCGA) database in April 2019. The EdgeR package was used to estimate differentially expressed miRNA between CRC tissues and normal tissues. |logFC| >1 and FDR <0.001 were deemed to be statistically significant. We also identified the cluster of differently expressed miRNAs and mRNAs based on the "pheatmap" package in R.

Prediction of miR-20a targets and enrichment analysis

The potential targets of miR-20a were identified based on the intersection of 3 online databases: miRTarBase [5], miRDB [6], and TargetScan [6]. Gene Ontology (GO) and Kyoto Encyclopedia of Genes and Genomes (KEGG) enrichment analyses were conducted using the clusterProfiler package [7]. The correlation between miR-20a and Foxj2 was assessed and plotted using the online starBase [8].

Tissue specimens and cell culture

Paired CRC tissues and its tumor-adjacent tissues were acquired from patients undergoing radical resection at the First People's Hospital of Jingmen from 2015 to 2016. We randomly selected 24 patients, and the study was approved by the Ethics Committee of the First People's Hospital of Jingmen.

The human CRC cell lines SW480, SW620, HCT-116, and HCT-8, as well as the normal intestinal epithelial cell line FHC, were obtained from the Cell Bank of the Chinese Academy of Sciences (Shanghai, China). RPMI-1640 (Gibco, Carlsbad, CA, USA) with 10% fetal bovine serum (FBS, Gibco) was used to culture the SW480 and HCT-8 cells in a humidified atmosphere with 5% CO_2 at 37°C. SW620 and HCT-116 cells were incubated in DMEM (Gibco) containing 10% FBS (Gibco) with the same conditions.

Western blot analysis

Total proteins were separated from the CRC tissues and cells. The concentrations of proteins were identified based on the Bio-Rad protein assay system (Bio-Rad, Hercules, CA, USA). SDS polyacrylamide gel electrophoresis (SDS-PAGE) was used to analyze the proteins, which were then transferred to PVDF membranes (Millipore). Then, the membrane proteins were subjected to immunoblotting with appropriate antibodies following the instructions of the manufacturer. The protein bands were visualized and quantified.

Indexed in: [Current Contents/Clinical Medicine] [SCI Expanded] [ISI Alerting System] [ISI Journals Master List] [Index Medicus/MEDLINE] [EMBASE/Excerpta Medica] [Chemical Abstracts/CAS]

Real-time quantitative PCR

TRIZOL reagent (Invitrogen) was used to isolate total RNA from frozen tumor tissues and cells. We used the cDNA Synthesis Kit (Takara, Tokyo, Japan) for synthesis of cDNA. The qPCR for miRNAs and mRNA was conducted with specific primers following the instructions of the manufacturer (Life Technologies, Carlsbad, CA, USA). QPCR results of miRNA and mRNA were expressed corresponding to U6 snRNA or β-actin mRNA, respectively. The sequences of the primers were:
Foxj2: 5'-TATGGTAGGGCATGAGGACAAC-3' (forward),
5'-GCAAACAATTAAAGGAGGACAAAC-3' (reverse);
β-actin: 5'-TAGTTGCGTTACACCCTTTCTTG-3' (forward),
5'-GCTGTCACCTTCACCGTTCC-3' (reverse);
miR-20a: 5'-ACACTCCAGCTGGGTAAAGTGCTTATAGTGCA-3' (forward),
5'-TGGTGTCGTGGAGTCG-3' (reverse);
U6: 5'-CTCGCTTCGGCAGCACA-3' (forward),
5'-AACGCTTCACGAATTTGCGT-3' (reverse).

Establishment and transfection of plasmid

The overexpression of miR-20a was performed by transfecting a miR-20a mimic with a synthesized double-stranded RNA oligonucleotide imitating the miR-20a precursor. The synthesized miR-20a mimic and the random negative control RNAs (control mimic and inhibitor) were obtained from GenePharma (Shanghai, China). For overexpression of endogenous Foxj2, the coding sequence of Foxj2 was amplified and subcloned into the pcDNA3.1(+) vector (Invitrogen, Carlsbad, CA, USA) according to the manufacturer' instructions. The empty plasmid was used as the negative control (control plasmid). The overexpressed plasmids were transfected into the cells by Lipofectamine 2000 (Invitrogen) based on the protocols.

Luciferase reporter assay

HCT-116 cells were seeded in 24-well plates with a density of 1×10^5 cells/well, which were further incubated for 24 h prior to transfection. When performing the reporter gene experiments, 0.5 μg of pGL3-Foxj2-3'UTR or pGL3-Foxj2-3'UTR Mut plasmid, 0.05 ng of the pRL-TK control vector (Promega, USA), and 100 nM miR-20a or the control RNA were used to collectively transfect the cells based on Lipofectamine 2000 (Invitrogen, USA). The Dual-Luciferase Reporter Assay kit (Promega) was used to explore the luciferase activities based on the instructions of the manufacturer. The normalization was assessed by the Renilla luciferase activity.

Transwell assay

Cell migratory and invasive capacities were determined by transwell chamber assay (BD Biosciences). The transfected cells were collected 24 h after transfection. Subsequently, 3.0×10^5 transfected cells or control cells were added to every upper insert in the serum-free medium. We added 500 μL culture medium supplemented with 10% FBS to the lower chamber. After the cultivation, non-migrated and non-invaded cells were discarded from the top surface of the transwell membrane using a cotton swab, and the cells remaining on the substrate were fixed with methanol, stained with 0.1% crystal violet, and photographed and counted. The above experiments were conducted in triplicate with biological samples.

Cell cycle analysis

Cell cycle analysis was conducted after 48 h of the miRNA transfection based on flow cytometry. Briefly, 2×10^6 cells were harvested and trypsinized, re-suspended in ethanol, and stored at 4°C for 15 min. Afterward, cells were centrifuged and re-suspended in 450 μL PBS and 50 μL RNase A at 37°C for 30 min. Cells were then treated with propidium iodide (PI, 50 μg/mL) and were cultured for 30 min in the dark at room temperature. Cell cycle analysis was achieved on a FACScan flow cytometer (BD Biosciences) using ModFit LT software.

Cell apoptosis

The Annexin V-FITC/PI staining kit (BD Biosciences, San Diego, CA, USA) was used for cell apoptosis. HCT-116 cells were seeded in 6-well plates with a density of 10^6 cells/mL. After transfecting for 24 h, Annexin V-FITC was used to label the cells for 20 min in the darkness. In total, 50 μg/mL of PI was added and further incubated for 30 min. Cell apoptosis was detected to calculate the percentage of cell death based on flow cytometry with the FACScan flow cytometer (BD Biosciences). All tests were performed in triplicate.

Cell proliferation and colony formation assay

For cell proliferation, cell viability was assessed by the MTT assay, in which 3.0×10^3 cells per well were seeded in 24-well plates and cultured in complete medium. Subsequently, cells were treated with 20 μL MTT (5 mg/mL) and cultured for 4 h. After discarding the medium, the formazan crystals were re-suspended in dimethylsulfoxide (DMSO) and the absorbance was immediately assessed using a microplate reader at 490 nm. For the colony formation assay, 1×10^3 cells were seeded in 6-well culture plates and cultured in complete culture medium. After culturing for 15 days, 3.7% methanol was applied to fix the colonies of living cells, 0.1% crystal violet was applied for staining, and cell colonies were counted. Colonies consisting of at least 50 cells were scored. All the above experiments were conducted in triplicate.

Indexed in: [Current Contents/Clinical Medicine] [SCI Expanded] [ISI Alerting System] [ISI Journals Master List] [Index Medicus/MEDLINE] [EMBASE/Excerpta Medica] [Chemical Abstracts/CAS]

Xenograft study

For *in vivo* analyses, cells (1×10^6) were suspended in 100 µL serum-free DMEM and subcutaneously injected into the flanks of BALB/c male nude mice (3–4 weeks old). For each group, 5 mice were included. The development of tumors in mice was observed every 3 days. Four weeks later, the mice were euthanized and the tumors were removed and photographed, and the volumes were calculated based on the following formula: length (mm)×width^2 (mm^2)/2.

Statistical analysis

Univariate Cox proportional hazards regression analysis was performed for the identification of candidate genes closely associated with survival. Of the screened genes, the candidates with *p*-value <0.001 were further subjected to multivariate Cox proportional hazards regression analysis to select the prognostic gene markers. SPSS 17.0 software (SPSS, Chicago, IL) was used for all the statistical analyses. The results are expressed as mean±standard deviation with no less than 3 biological repeats. The comparison between the 2 groups was performed by *t* test. One-way ANOVA was used to assess the significance of variations in different groups. *P*-values <0.05 were deemed to be statistically significant.

Results

miR-20a was overexpressed in CRC and upregulated cell proliferation and colony formation

The statistical software R and EdgeR packages were used to identify the differentially expressed microRNAs between control and tumor tissues. Figure 1A displays the volcano plot. All of the altered miRNAs expressed in CRC tissues were identified (Figure 1B), showing that the expression of miR-20a was higher in CRC. RT-qPCR analysis showed that the levels of miR-20a were elevated in 4 CRC cell lines – SW480, SW620, HCT-8, and HCT-116 – compared with the normal cell line FHC (Figure 1C). Additionally, it was revealed in Figure 1D that the level of miR-20a expressed in CRC tissues was higher in CRC tissues than in the relevant para-carcinoma tissues.

To further explore the roles of miR-20a in the development of CRC, MTT and colony formation assays were performed *in vitro*. miR-20a was overexpressed in HCT-116 cells transfected with miR-20a mimics (Figure 1E). MTT assay showed that cell proliferation was facilitated by overexpression of miR-20a (Figure 1F). Colony formation assay showed that overexpression of miR-20a facilitated the colony-forming ability of HCT-116 cells (Figure 1G). The number of colonies developed from cells treated with miR-20a mimics was counted, which was dramatically higher than that of scramble or control cells (* P<0.05).

Identification of miR-20a candidate target genes

To assess the abnormal regulation of miR-20a on CRC, the potential mRNA targets of miR-20a were obtained by the verified target module of miRDB, miRTarBase, and TargetScan databases. Eventually, 120 candidates were selected from these 3 databases. Univariate Cox regression analysis and stepwise multivariate Cox regression analysis were performed to assess the relationship between differentially expressed genes and the overall survival of patients with CRC. As represented in Supplementary Table 1, 228 downregulated genes with *p*-value <0.001 were considered as the prognostic candidates, which were chosen for the next screening. To authenticate the reliable target genes, the intersection of promising miR-20a target genes and 228 reduced differentially expressed genes were extracted, which eventually screened out 3 target genes (FOXJ2, CRY2, and PLS1), among which, FOXJ2 has never been previously studied in CRC (Figure 2A).

We assessed the correlation between miR-20a and the candidates using the combination of GO analysis and KEGG pathway analysis. GO enrichment results (Figure 2B) suggested that the activation of MAPKK was the most enriched pathway. The KEGG results (Figure 2C) suggested that the candidates are generally involved in development of a variety of cancers and EGFR tyrosine kinase inhibitor resistance. Moreover, we also developed the expression heatmap for all potential target genes of miR-20a (Figure 2D). The GEPIA database also verified that the Foxj2 expression was inhibited in tumors in comparison with normal tissues (Figure 2E). The results of starBase (Figure 2F) suggested that the level of Foxj2 was negatively correlated with that of miR-20a.

Foxj2 serves as the direct target of miR-20a in CRC cells

To sequentially identify the putative target gene of miR-20a in CRC, Foxj2 was utilized as a possible target gene of miR-20a (Figure 3A). To further confirm Foxj2 as a target of miR-20a, the miR-20a binding site was speculated to be in the 3'UTR of Foxj2 mRNA, which was cloned into the dual-luciferase reporter vector. Subsequently, either miR-20a or the negative control RNA with the dual-luciferase expression vector including wild-type or mutant 3'UTR fragment of Foxj2 was co-transfected. Dual-luciferase reporter assay was performed to validate that the luciferase activity of the wild-type Foxj2 3'-UTR luciferase complex rather than the mutant Foxj2 3'UTR was dramatically suppressed by the overexpressed miR-20a (Figure 3B) (P<0.05). The above results show that Foxj2 directly interacts with miR-20a. In addition, miR-20a was transfected to the HCT-116 cells, and the results of Western blot analyses proved

Indexed in: [Current Contents/Clinical Medicine] [SCI Expanded] [ISI Alerting System] [ISI Journals Master List] [Index Medicus/MEDLINE] [EMBASE/Excerpta Medica] [Chemical Abstracts/CAS]

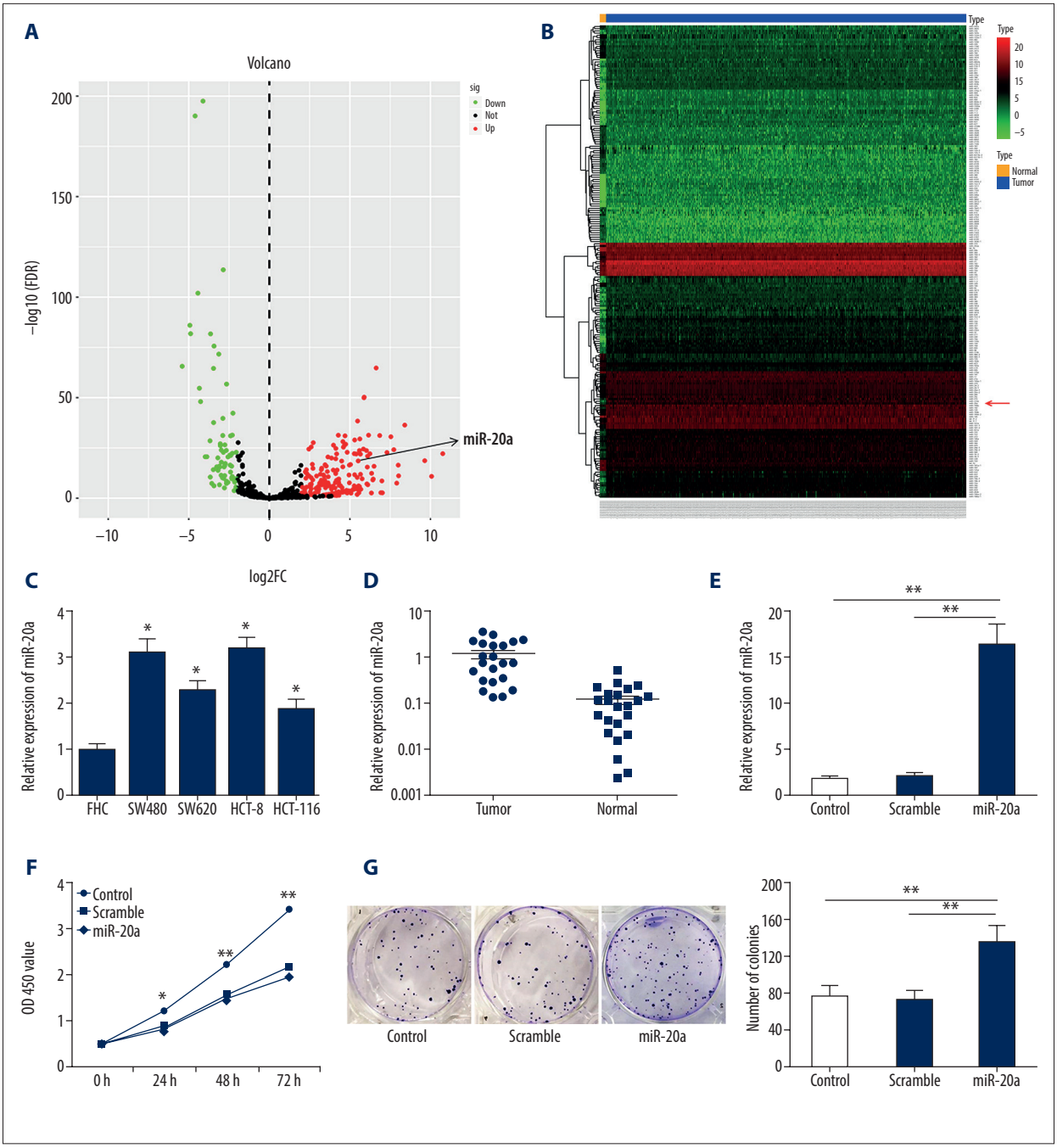

Figure 1. miR-20a expression was upregulated in CRC and overexpression of miR-20a promoted cell growth and colony formation. (**A**) Volcano plot of differentially expressed miRNAs. X-axis: $\log_2$ (fold change); Y-axis: $\log_{10}$ (FDR). Red dots: significantly upregulated genes; Green dots: significantly downregulated genes; Black dots: non-differentially expressed genes. (**B**) The heatmap of the differentially expressed miRNAs between CRC tissues and adjacent normal tissues. Differentially expressed genes in CRC were screened and are presented in the rows, and the columns are samples. The green represents downregulation, while a red represents upregulation. (**C**) The expression of miR-20a was detected in CRC cell lines (SW480, SW620, HCT-8, and HCT-116) and the normal cell line FHC using qPCR analysis. (**D**) qPCR analysis of miR-20a expression levels in 24 pairs of CRC tissues and their corresponding adjacent normal tissues (P<0.001). (**E**) qPCR analysis was used to evaluate miR-20a expression after transfection with miR-20a mimics or scramble or no transfection (control). (**F**) MTT assay was used to study the proliferation of the HCT-116 cells after transfection with the miR-20a mimics or scramble or control. (**G**) Overexpression of miR-20a promoted the HCT-116 cells colony formation. The relative numbers of colonies are shown in the right. * P<0.05; ** P<0.001.

Indexed in: [Current Contents/Clinical Medicine] [SCI Expanded] [ISI Alerting System] [ISI Journals Master List] [Index Medicus/MEDLINE] [EMBASE/Excerpta Medica] [Chemical Abstracts/CAS]

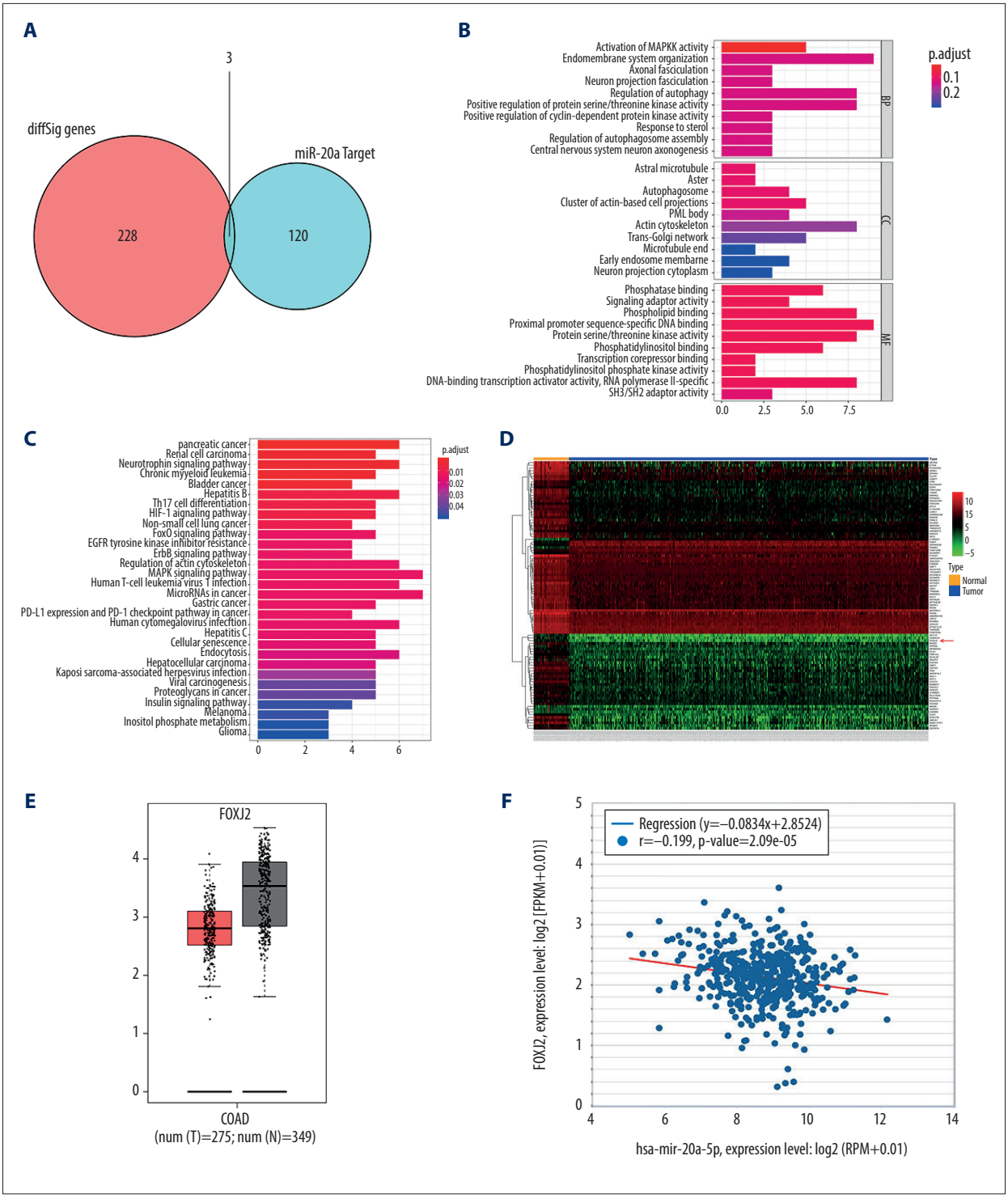

Figure 2. FOXJ2 was predicted to be the target of miR-20a by bioinformatics analysis. (**A**) Venn diagram of 3 overlapping DEGs from differentially expressed mRNAs and predicted miR-20a target genes. (**B, C**) GO analysis and KEGG pathway of predicted miR-20a target genes are shown diagrammatically. (**D**) The heatmap of the predicted miR-20a target genes. Red: high expression level; green: low expression level. (**E**) The expression level of FOXJ2 was validated according to the GEPIA database. (**F**) A significant negative correlation was found between FOXJ2 and miR-20a expression.

Indexed in: [Current Contents/Clinical Medicine] [SCI Expanded] [ISI Alerting System] [ISI Journals Master List] [Index Medicus/MEDLINE] [EMBASE/Excerpta Medica] [Chemical Abstracts/CAS]

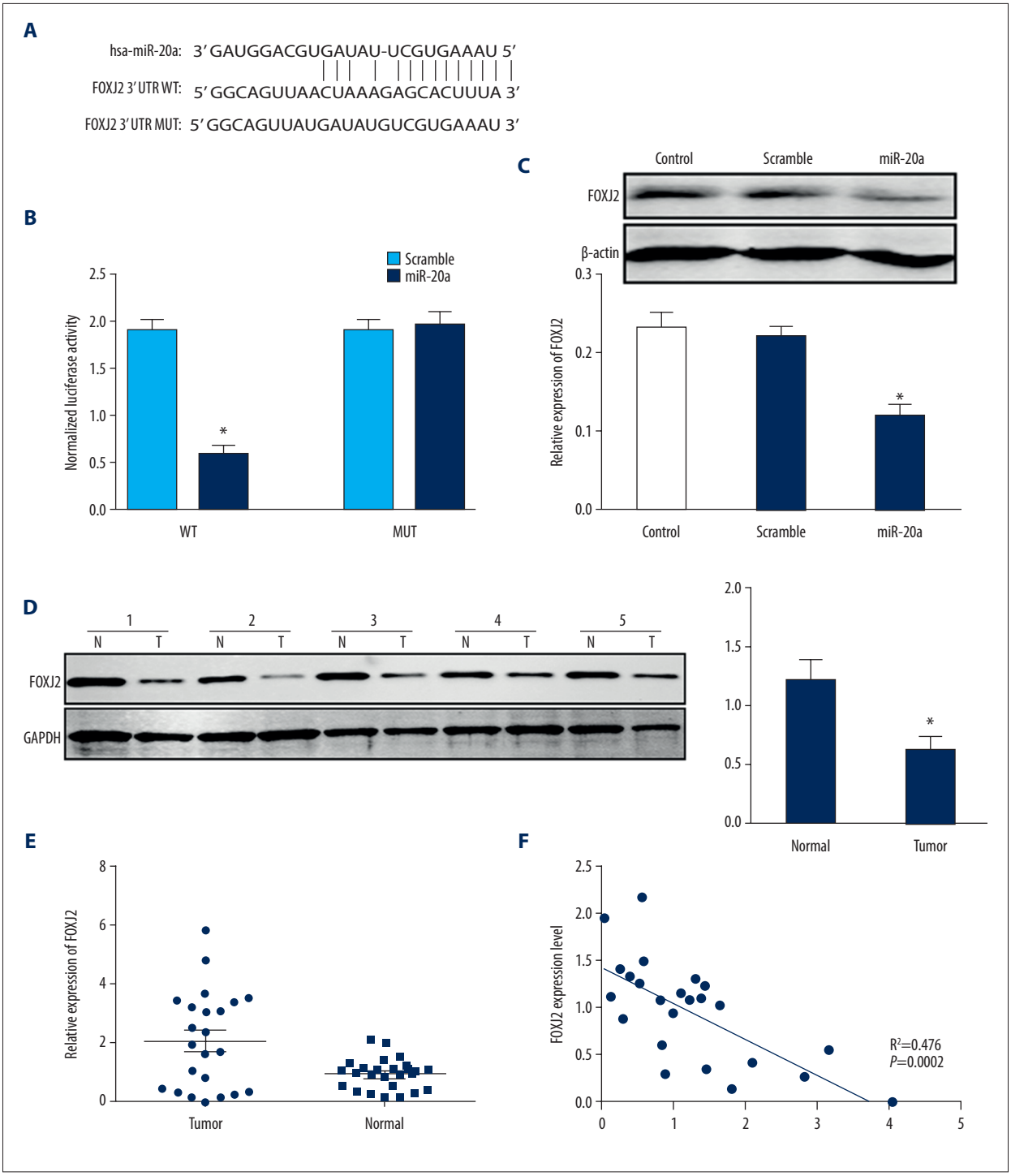

Figure 3. Foxj2 is a direct target gene of miR-20a in CRC cells. (**A**) The sequences of miR-20a binding sites within the human Foxj2 3'UTR and schematic reporter constructs. Foxj2-WT represents the reporter constructs containing the entire 3'UTR sequences of Foxj2. Foxj2-MUT represents the reporter constructs containing mutated nucleotides. (**B**) Analysis of relative luciferase activities of Foxj2-WT and Foxj2-MUT. (**C**) Western blot analysis showed that overexpression of miR-20a downregulated the Foxj2 protein level in the HCT-116 cells. (**D**) The expression of Foxj2 protein levels in CRC tissues was established by Western blot (representative results of 5 cases were shown). (**E**) qPCR analyses of Foxj2 expression in CRC and matched adjacent normal tissues. (**F**) The relationship between miR-20a and Foxj2 expression was evaluated by Spearman's correlation analysis of CRC tissues (R^2=0.476, P<0.001). * P<0.05.

Indexed in: [Current Contents/Clinical Medicine] [SCI Expanded] [ISI Alerting System] [ISI Journals Master List] [Index Medicus/MEDLINE] [EMBASE/Excerpta Medica] [Chemical Abstracts/CAS]

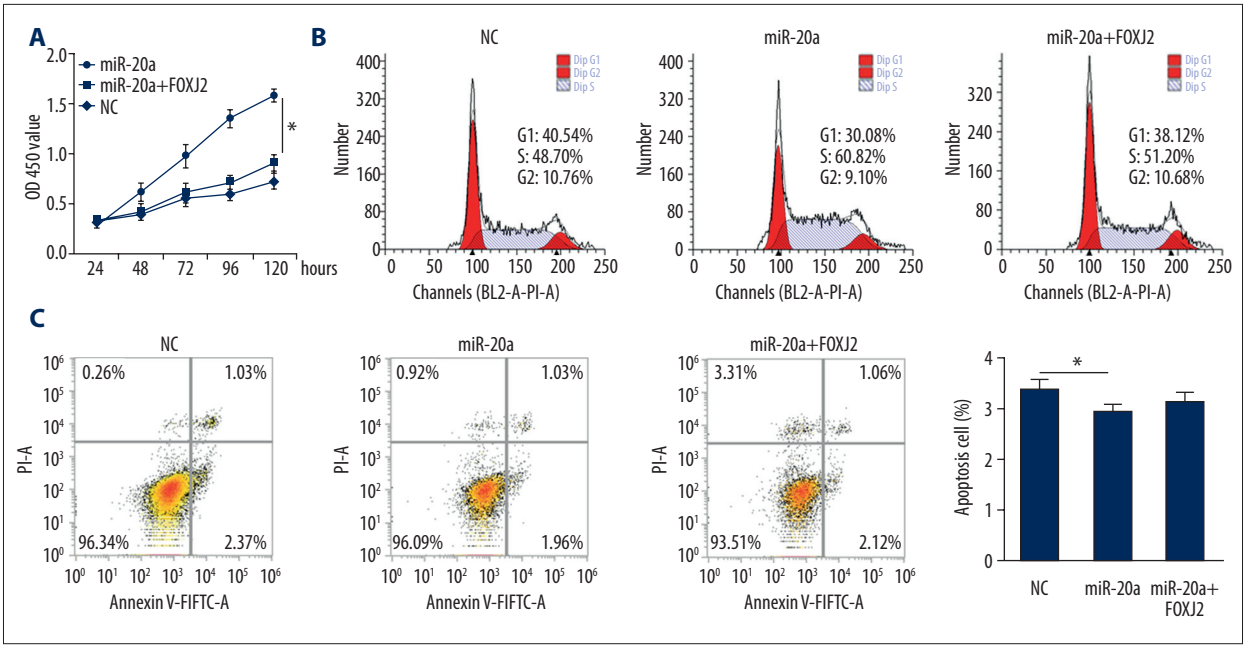

Figure 4. Effects of Foxj2 overexpression on miR-20a-mediated CRC progression. (**A**) MTT analysis was used to detect cell proliferation at various time points after transfection with miR-20a mimic and Foxj2 overexpression plasmid. (**B, C**) Cell cycle and cell apoptosis of HCT-116 cells transfected with miR-20a with and without Foxj2 overexpression were assessed by flow cytometry. * P<0.05.

that the miR-20a treatment markedly inhibited Foxj2 expression at the protein level, as indicated in Figure 3C.

Additionally, we performed Western blot and qPCR assays to validate the levels of Foxj2 protein and mRNA in 24 freshly collected CRC tissues and para-carcinoma tissues. Foxj2 was found to be markedly downregulated in 18 of the 24 cases, in contrast to the para-carcinoma tissues (P<0.05); Figure 3D shows 5 representative pairs. In comparison with the corresponding para-carcinoma tissues, underexpression of Foxj2 mRNA was observed in the CRC tissues based on qPCR analysis (P<0.05) (Figure 3E). Furthermore, the expression of Foxj2 was negatively correlated with miR-20a expression (Figure 3F).

Foxj2 partially reversed the effects of miR-20a-mediated CRC progression

To verify whether miR-20a exerted a biological role in CRC progression via targeting Foxj2, HCT-116 cells were collectively transfected with miR-20a mimics and the Foxj2-overexpressed plasmid. As represented in Figure 4A, the MTT assay indicated that the miR-20a-mediated HCT-116 cell proliferation could be reversed by overexpressed Foxj2. Furthermore, it was indicated in Figure 4B that the upregulated Foxj2 expression partially alleviated the effects of the miR-20a-accelerated S phase and induced cell cycle arrest at the G1 stage. Furthermore, Figure 4C revealed the results of flow cytometry analysis, indicating that the apoptosis rate of HCT-116 cells was inhibited by miR-20a mimics and miR-20a with Foxj2-overexpressed plasmid in contrast to the NC group (P<0.05).

Colony formation and transwell assays revealed that the promotional roles of miR-20a on cell growth, migration, and invasion of HCT-116 cells could be reversed by the overexpression of Foxj2 (Figure 5A, 5B). It was demonstrated in Figure 5C that the reversion of the impacts of miR-20a in tumor development of HCT-116 cells *in vivo*. GO and KEGG enrichment analysis results also suggested that the positively regulated EGFR/AKT pathway induced by miR-20a could be inhibited by the overexpression of Foxj2, indicating that the signaling pathway proteins could serve as the downstream regulation factors of Foxj2 (Figure 5D). Overall, our results suggest that the progression of CRC cells was promoted by miR-20a via modulating Foxj2 *in vitro* and *in vivo*.

Discussion

miR-20a is a member of the miR-17-92 group and is located in the 13q31.1 region. Sequencing data demonstrated that the level of miR-20a was dramatically higher in the CRC cells than in the normal cells, suggesting that miR-20a is positively associated with cell proliferation and colony formation. GO analysis and KEGG pathway analysis showed that Foxj2, as the tumor suppressor gene, targeted miR-20a in CRC. Further research shows that there is a binding site of the 3' UTR of Foxj2 with

Indexed in: [Current Contents/Clinical Medicine] [SCI Expanded] [ISI Alerting System] [ISI Journals Master List] [Index Medicus/MEDLINE] [EMBASE/Excerpta Medica] [Chemical Abstracts/CAS]

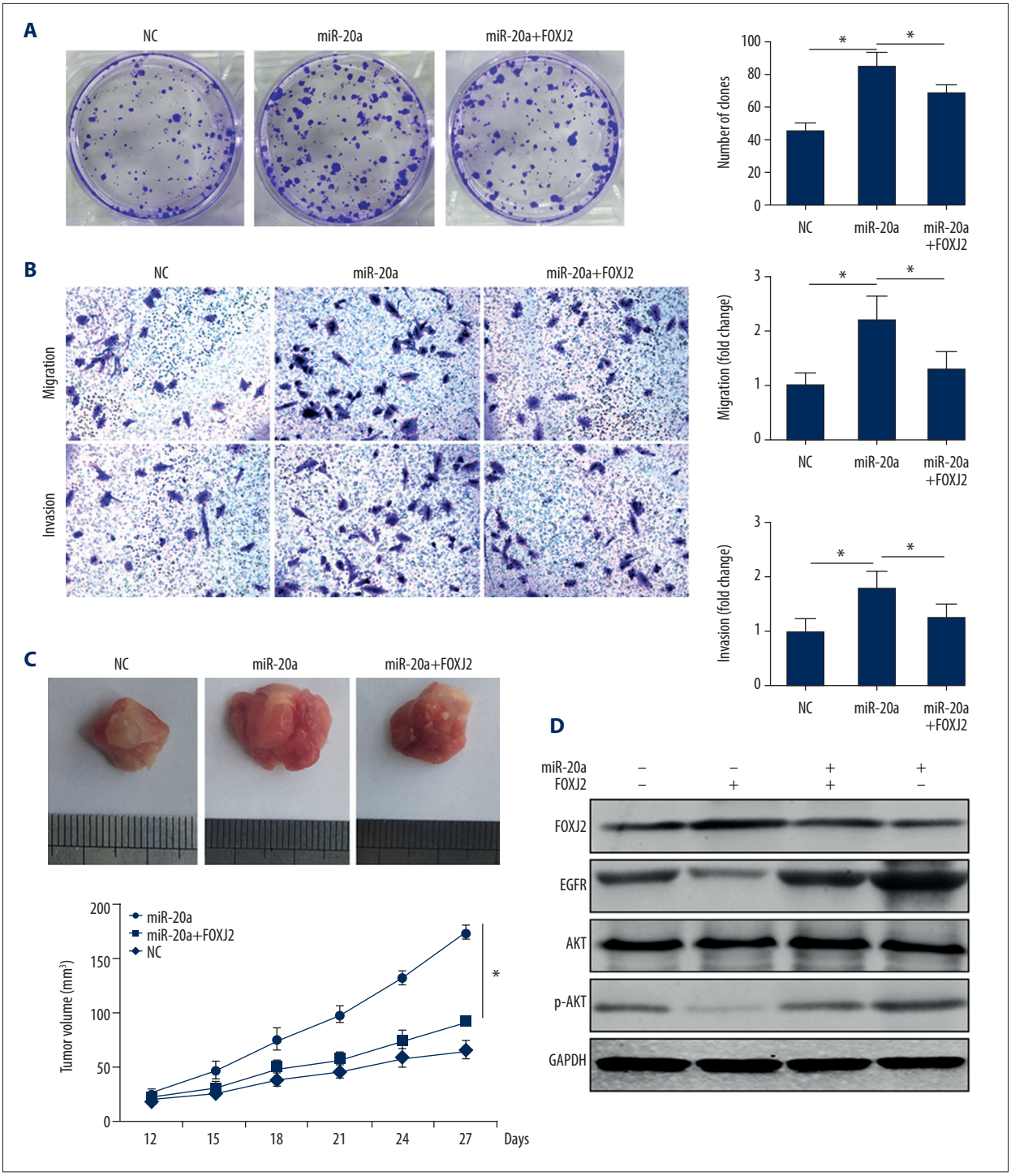

Figure 5. The effects of miR-20a-promoted CRC cell proliferation, migration, and invasion were mediated by the downregulation of Foxj2 *in vitro* and *in vivo*. (**A**) Colony formation assays were used to determine the effects of growth in HCT-116 cells transfected with miR-20a with and without Foxj2 overexpression. The number of colonies was analyzed quantitatively. (**B**) Cell migration and invasion were performed in HCT-116 cells transfected with miR-20a with and without Foxj2 overexpression. Representative images of migrated and invaded cells (magnification ×100) and quantification of migrated and invaded cells per field. (**C**) The proliferation activity of xenograft tumors in HCT-116 cells transfected with miR-20a and Foxj2 overexpression on the average volumes in xenograft tumors. (**D**) The effects of Foxj2 overexpression on the expression of EGFR/AKT signaling pathway proteins in miR-20a-transfected HCT-116 cells were tested by Western blot analysis. * P<0.05.

Indexed in: [Current Contents/Clinical Medicine] [SCI Expanded] [ISI Alerting System] [ISI Journals Master List] [Index Medicus/MEDLINE] [EMBASE/Excerpta Medica] [Chemical Abstracts/CAS]

miR-20a in CRC. Analyses of miR-20a and Foxj2 protein expression levels in human CRC tissues were negatively associated with each other. Flow cytometry analysis showed that the overexpressed Foxj2 participates in the regulation of CRC development by miR-20a. By decreasing the Foxj2 levels, miR-20a facilitates the proliferation of colorectal cells, but the flow pattern suggests that miR-20a/Foxj2 does not play a in apoptosis *in vivo*. Further, *in vitro* and *in vivo* experiments have revealed that overexpression of Foxj2 can effectively reverse the cancer-promoting effects of miR-20a. The above data broadened the horizon for the new regulatory network targeted miR-20a and Foxj2 in CRC, and show the specific mechanism by which miR-20a promotes CRC.

Previous research reported that miR-20a was decreased in several solid tumors, like breast cancer [9] and pancreatic carcinoma [10], but miR-20a is a broadly overexpressed oncogene in various tumors, including anaplastic thyroid cancer [11], lung cancer [12], prostate cancer [13], esophageal squamous cell carcinoma [14], gliomas [15], and colon adenocarcinoma [16], suggesting that the expression and role of miR-20a vary in different tumor types. It has been clearly indicated that the abilities of cell proliferation, invasion, and tumor metastasis in breast cancer cells are suppressed by overexpression of miR-20a [17]. In contrast, miR-20a was observed to inhibit the proliferation and metastasis of the cells of pancreatic carcinoma via directly reducing Stat3 [10]. Other reports indicated that overexpression of miR-20a facilitates the proliferation of ovarian cancer cells and the migration and invasion in the cells of cervical cancer, ovarian cancer and osteosarcoma [18–20], implying that miR-20a acted as the onco-miR. The present study demonstrates that miR-20a is upregulated in CRC tissues, which agrees with the combined detection of TCGA and validation of qPCR. Additionally, miR-20a increased the proliferation and colony-forming ability of CRC cells. Hence, it may be concluded that the deregulation of miR-20a functions as a carcinogenic miRNA and is involved in the progression of CRC. Previous studies showed the crucial effects of miRNAs on the genesis and progression of tumors through regulating the levels of target genes [21]. To verify the bioinformatics analysis for predicting the potential biomarkers of CRC, the screened candidate gene Foxj2 was further validated. Our data also proved that Foxj2 was directly targeted to miR-20a in the CRC cells.

The genes associated with differentiation, apoptosis, proliferation, metabolism, migration, and invasion were reported to be modulated by the Forkhead box (FOX) transcription factor family [22,23]. Forkhead box j2 (Foxj2), belonging to the Forkhead box transcription factor family [24], which exists in several mammals and other vertebrates [25–27], is widely distributed in different organs and tissues of adults and in fetuses. More importantly, recent studied showed that Foxj2 may participate in tumorigenesis [28]. Foxj2 regulates the process of cell migration and cell cycle [29,30]. For example, some observations indicated that elevated Foxj2 inhibits cell migration and invasion of glioma and is positively associated with E-cadherin [31]. In addition, Foxj2 may contribute to the development of EMT via the Notch signaling pathway in non-small cell lung cancer [32]. In the present work, integrated bioinformatics analyses and experiments showed that Foxj2 serves as a tumor inhibitor in CRC. In line with the above results, we found that the migration and invasion of CRC is facilitated by miR-20a via inhibiting Foxj2. These findings show the strong correlation between miR-20a and the Foxj2 axis, which has a significant impact on cell proliferation and tumorigenesis.

Conclusions

This is the first study to demonstrate that CRC tumorigenesis is promoted by targeting of miR-20a with Foxj2. Further results on miR-20a/Foxj2 axis will offer a promising target and open the way for new CRC molecular therapeutics. Nevertheless, it is not clear how Foxj2 influences CRC progression. Hence, further studies are needed to elucidate the effects and functions of Foxj2 in CRC cells.

Conflict of interest

None.

Indexed in: [Current Contents/Clinical Medicine] [SCI Expanded] [ISI Alerting System] [ISI Journals Master List] [Index Medicus/MEDLINE] [EMBASE/Excerpta Medica] [Chemical Abstracts/CAS]

Supplementary Data

Supplementary Table 1. Prognostic value of the target genes in CRC patients of the TCGA cohort.

Gene symbol	Univariate analysis		Multivariate analysis	
	HR	P-value	HR	P-value
ZNF133	1.537498631	0.008697705	38	<0.001
ZKSCAN2	1.691982256	0.004876581	8.9	<0.001
ZDHHC11	1.183004595	0.006286627	3.2e-01	<0.001
WSB2	0.467109344	0.003950621	25	<0.001
WDR86	1.40240492	0.006044641	72	<0.001
VDAC1	0.531016786	0.006341117	2.7e-03	<0.001
USH1G	1.260619617	0.001234788	2.1	<0.001
TRIM25	0.573345214	0.007816236	2.2e-01	<0.001
TREX2	1.373224848	0.002772185	16	<0.001
TRABD2B	1.285006739	0.002930684	6.0e-01	<0.001
TMEM81	1.644187505	0.008760967	1.6e-01	<0.001
ZKSCAN2	1.691982256	0.004876581	8.9	<0.001
ZDHHC11	1.183004595	0.006286627	3.2e-01	<0.001
WSB2	0.467109344	0.003950621	25	<0.001
WDR86	1.40240492	0.006044641	72	<0.001
VDAC1	0.531016786	0.006341117	2.7e-03	<0.001
USH1G	1.260619617	0.001234788	2.1	<0.001
TRIM25	0.573345214	0.007816236	2.2e-01	<0.001
TREX2	1.373224848	0.002772185	16	<0.001
TRABD2B	1.285006739	0.002930684	6.0e-01	<0.001
TMEM81	1.644187505	0.008760967	1.6e-01	<0.001
TMEM165	0.586600114	0.007386349	1.1e-02	<0.001
TMCC2	1.576746915	0.000688545	8.9e-02	<0.001
TINAG	0.862994088	0.00425559	2.9e-01	<0.001
TGM6	1.219997455	0.004782644	5.1e-01	<0.001
TCF7L1	1.520206387	0.000495012	5.9	<0.001
TCEAL5	1.213662999	0.004119467	3.7e-01	<0.001
TCAIM	0.572670505	0.003588079	1000	<0.001
SUSD5	1.232270257	0.003620369	5.0e-01	<0.001
STK32C	1.40872781	0.005501541	8.4e-02	<0.001
SRPX	1.241306378	0.001854167	2.9	<0.001
SOX7	1.372226734	0.003493233	1.1e-01	<0.001
SOWAHA	0.738552315	0.000853741	3.4e-01	<0.001
SNCB	1.457793587	1.65609E-05	7.1	<0.001
SLITRK2	1.251506902	0.001222424	5.3e-01	<0.001

Indexed in: [Current Contents/Clinical Medicine] [SCI Expanded] [ISI Alerting System] [ISI Journals Master List] [Index Medicus/MEDLINE] [EMBASE/Excerpta Medica] [Chemical Abstracts/CAS]

Gene symbol	Univariate analysis		Multivariate analysis	
	HR	P-value	HR	P-value
SLC6A17	1.288351213	0.00255427	6.1e-01	<0.001
SLC38A8	1.288767274	0.00473397	1.7	<0.001
SLC28A2	0.88596792	0.006146815	2	<0.001
SLC20A2	0.63283218	0.009266251	6.6e-02	<0.001
SLC16A8	1.352969047	0.00026993	2.7e-01	<0.001
SIX2	1.162090077	0.001996522	2.6	<0.001
SIN3B	1.914175669	0.007211485	7.5	<0.001
SHQ1	0.45559615	0.009472777	35	<0.001
SH3GL3	1.352516953	0.003004732	1.6e-01	<0.001
SH3D19	0.656860309	0.00634363	3.0e-01	<0.001
SGK2	0.83804645	0.00294523	2.7e-01	<0.001
SEZ6L2	1.435716471	0.001675202	8.2	<0.001
SEMA6C	1.610116899	0.000195179	4.8	<0.001
SCN3B	1.215243964	0.005809295	3.5e-01	<0.001
SBK2	1.681191002	4.28891E-05	1.1e-01	<0.001
SACS	1.295055049	0.009934617	4	<0.001
S100P	0.847861221	0.004546645	4.0e-01	<0.001
RUBCNL	0.854620542	0.007175531	5	<0.001
RTN4RL2	1.262078269	0.009330644	3.4e-01	<0.001
RTL5	1.305462946	0.004553238	75	<0.001
RORC	0.810066461	0.004513852	6.7e-01	<0.001
RNF43	0.794265928	0.003920463	1.0e-01	<0.001
RBP7	1.409275162	0.000394274	2.3e-01	<0.001
RBM3	0.676121381	0.008539379	1.3e-01	<0.001
RBM17	2.414924435	0.007712655	6800	<0.001
QRICH2	1.481967745	0.002424447	5.8	<0.001
PTH1R	1.271139463	0.001344702	3.8	<0.001
PRRT4	1.200187997	0.001213094	3.6e-01	<0.001
PRRT1	1.376312756	0.009195431	8.1	<0.001
PRELID2	0.639356718	0.002758224	32	<0.001
PPP2CB	0.591469544	0.009534317	2.7e-03	<0.001
PPFIA4	1.293115792	0.003103059	8.4	<0.001
PPARGC1A	0.834950723	0.001527893	1.9e-01	<0.001
POFUT2	2.049110498	0.005309024	3.2e-02	<0.001
PMM2	0.437645266	0.000311294	3000	<0.001
PMCH	0.643781405	0.003027112	2.2e-01	<0.001
PLS1	0.666294786	0.00375481	6.7	<0.001
PLPP2	0.641212973	0.001072941	7.6e-04	<0.001

Indexed in: [Current Contents/Clinical Medicine] [SCI Expanded] [ISI Alerting System] [ISI Journals Master List] [Index Medicus/MEDLINE] [EMBASE/Excerpta Medica] [Chemical Abstracts/CAS]

Gene symbol	Univariate analysis		Multivariate analysis	
	HR	P-value	HR	P-value
PLEKHG4B	1.302343681	0.000505889	1.1e-01	<0.001
PIP5K1C	1.716568911	0.006747328	2.6e-01	<0.001
PDZD4	1.17293216	0.007277794	2.3	<0.001
PDE1B	1.316236541	0.002107239	2.6e-01	<0.001
PDCD6IP	0.554647065	0.009870352	260	<0.001
PCDHB8	1.143959444	0.008713351	5.5e-01	<0.001
PAGE1	1.173634426	0.004839683	2.9e-01	<0.001
OVOL3	1.315953982	0.008292592	1.6	<0.001
OR2B6	1.299546249	0.009721983	6.9e-01	<0.001
OAZ2	2.842306103	0.002254038	110	<0.001
NXPE3	1.434379996	0.008906926	8.2e-03	<0.001
NPTXR	1.209880744	0.002997987	3.8e-01	<0.001
NPR2	1.585561158	0.005736431	1.8e-02	<0.001
NPR1	1.267838515	0.008905722	1.8e-01	<0.001
NLGN1	1.176341275	0.001783991	2.5	<0.001
NHLRC4	1.551869878	0.000643194	74	<0.001
NGFR	1.200989542	0.001532476	1.4e-01	<0.001
NGF	1.318819479	0.004309054	2.5e-01	<0.001
NFATC1	1.307619018	0.007598954	46	<0.001
NECAB2	1.27076126	0.006135428	4.9	<0.001
NCKAP5L	2.169171268	2.56373E-05	3.1e-02	<0.001
NAT1	0.73284881	0.006734646	3.9	<0.001
NACAD	1.305822623	0.00141327	48	<0.001
MYB	0.630652971	0.002410283	4.9e-01	<0.001
MMAA	0.576201489	0.001516101	2.9	<0.001
MLLT11	1.34614653	0.006077126	26	<0.001
MKRN2OS	0.654012218	0.001024618	1.6e-01	<0.001
METTL9	0.538908907	0.009335042	1.3e-01	<0.001
MC1R	1.29905193	0.006969694	1.4e-01	<0.001
MAPKAPK5	0.470290813	0.00753356	490	<0.001
MAPK12	1.3737705	0.00094184	18	<0.001
MAGEF1	1.956272182	0.007680343	3.4e-04	<0.001
MAGEA1	1.247064893	2.7493E-05	3.3	<0.001
LRP2	1.288962734	6.10532E-05	1.5	<0.001
LINGO1	1.355302198	0.000399767	4.6e-01	<0.001
LEP	1.18500816	0.002465145	12	<0.001
MMAA	0.576201489	0.001516101	2.9	<0.001
MLLT11	1.34614653	0.006077126	26	<0.001

Indexed in: [Current Contents/Clinical Medicine] [SCI Expanded] [ISI Alerting System] [ISI Journals Master List] [Index Medicus/MEDLINE] [EMBASE/Excerpta Medica] [Chemical Abstracts/CAS]

Gene symbol	Univariate analysis		Multivariate analysis	
	HR	P-value	HR	P-value
MKRN2OS	0.654012218	0.001024618	1.6e-01	<0.001
METTL9	0.538908907	0.009335042	1.3e-01	<0.001
MC1R	1.29905193	0.006969694	1.4e-01	<0.001
MAPKAPK5	0.470290813	0.00753356	490	<0.001
MAPK12	1.3737705	0.00094184	18	<0.001
MAGEF1	1.956272182	0.007680343	3.4e-04	<0.001
MAGEA1	1.247064893	2.7493E-05	3.3	<0.001
LRP2	1.288962734	6.10532E-05	1.5	<0.001
LINGO1	1.355302198	0.000399767	4.6e-01	<0.001
LEP	1.18500816	0.002465145	12	<0.001
KCNIP3	1.260837142	0.004916884	4.7e-02	<0.001
ITIH6	1.209106013	0.002657523	7.3	<0.001
ITGA5	1.307298059	0.005855555	990	<0.001
IRX6	1.322112702	0.000843443	3.3e-01	<0.001
IQSEC3	1.27677672	0.004666794	1.9e-01	<0.001
INHBB	1.177779802	0.004605681	31	<0.001
HTR2C	1.227695273	0.002343627	3.7	<0.001
HRASLS5	1.169770556	0.008070109	5.0e-01	<0.001
HPD	1.334359324	0.004019401	2.3	<0.001
HPCAL4	1.283814727	0.00451649	6.7	<0.001
HOXC6	1.181620432	0.000133735	3.3e-01	<0.001
HOXC13	1.204636727	0.000531529	2.5	<0.001
HEYL	1.676211788	0.000538317	4.5	<0.001
HEY1	1.587051358	0.002290132	2.4e-01	<0.001
HEXB	0.461726956	0.000952528	120000	<0.001
HDAC7	1.96210524	0.006035858	110000	<0.001
GSPT1	0.489079951	0.005568086	1.2e-05	<0.001
GRIK5	1.183858849	0.008746472	5.7e-01	<0.001
GRID1	1.336945729	0.00449767	3.1	<0.001
GPRC5B	1.535508947	0.000501917	13	<0.001
GPRASP1	1.272720263	0.006263557	6.4e-02	<0.001
GPR156	1.308364429	0.001153267	4.2	<0.001
GLYATL1	0.860613222	0.006528162	9.5e-02	<0.001
GDF15	0.833412966	0.008604588	1.4	<0.001
GAREM2	1.381779663	0.005033009	1.6	<0.001
GALNT15	1.204296146	0.008635526	1.4e-01	<0.001
FZD4	1.486653675	0.006249553	3.6e-03	<0.001
FSTL3	1.271624144	0.007962522	1.6e-01	<0.001

Indexed in: [Current Contents/Clinical Medicine] [SCI Expanded] [ISI Alerting System] [ISI Journals Master List] [Index Medicus/MEDLINE] [EMBASE/Excerpta Medica] [Chemical Abstracts/CAS]

Gene symbol	Univariate analysis		Multivariate analysis	
	HR	P-value	HR	P-value
FOXL2NB	1.345119444	5.39726E-05	4.2	<0.001
FOXL2	1.259891809	0.000933203	6.9e-01	<0.001
FOXJ2	2.472932089	0.002849779	1.9e-01	<0.001
FOXD4	1.245464377	0.005531115	3.8	<0.001
FOXC1	1.270115339	0.002834468	5.4e-01	<0.001
FNDC5	1.332360452	0.001709798	2.6	<0.001
FLT3LG	1.417336731	0.009536758	1.8e-02	<0.001
FES	1.443664395	0.005175721	3.0e-01	<0.001
FAM117A	1.562351037	0.009158748	400	<0.001
FAM110D	1.383624103	0.002865335	8.1	<0.001
FADS1	1.287690981	0.006909719	1.9	<0.001
FABP4	1.139559679	0.001160698	4.1e-01	<0.001
EXTL1	1.265980039	0.005035667	1.0e-01	<0.001
ETS2	0.668284016	0.005916623	7.1	<0.001
ERMAP	0.568400341	0.009071429	2.3e-02	<0.001
ERICH3	1.230607448	0.006719883	1.9	<0.001
EREG	0.887017859	0.006138749	1.5	<0.001
EPS8	0.583792225	0.006078897	2.8	<0.001
EPO	1.377559357	0.008650002	6.7	<0.001
EPHB2	0.722678923	0.009896647	35	<0.001
EMC3	0.431853091	0.001771981	23	<0.001
EIF2S3B	0.78869205	0.003802776	5.2e-01	<0.001
EFHD1	1.390626574	0.001678327	5	<0.001
EBF4	1.460934784	0.000259432	4.2	<0.001
DRD4	1.302006231	0.004539947	60	<0.001
DOCK3	1.289854413	0.002209175	3.0e-01	<0.001
DMPK	1.427657686	0.002350812	4.0e-01	<0.001
DLG4	1.479923277	0.00994533	1.1e-01	<0.001
DHX15	0.392830659	0.000995095	2400	<0.001
DCTN1	2.095513206	0.007449317	1.1e-05	<0.001
CYP4F12	0.741142308	0.000753205	3.7	<0.001
CTNNA1	0.519488852	0.000584074	36	<0.001
CTF1	1.248947118	0.007277252	7.2e-01	<0.001
EPHB2	0.722678923	0.009896647	35	<0.001
CT45A1	1.285770132	0.00881524	4.3e-02	<0.001
CRY2	1.862665669	0.003229067	2.9e-02	<0.001
CRISPLD2	1.347498521	0.008331665	1.9e-01	<0.001
CORO6	1.314726218	0.002462567	2.1e-01	<0.001

Indexed in: [Current Contents/Clinical Medicine] [SCI Expanded] [ISI Alerting System] [ISI Journals Master List] [Index Medicus/MEDLINE] [EMBASE/Excerpta Medica] [Chemical Abstracts/CAS]

Gene symbol	Univariate analysis		Multivariate analysis	
	HR	P-value	HR	P-value
CNTNAP1	1.297543992	0.008474966	3.0e-01	<0.001
CNPY1	1.279382847	0.005932603	2.4	<0.001
CLSTN3	1.648521955	0.004361652	68	<0.001
CLRN3	0.690451251	0.000104942	18	<0.001
CILP	1.116653758	0.00881835	4.6e-01	<0.001
CIDEA	1.157068648	0.004837007	2.2	<0.001
CHDH	0.720216727	0.008461958	3.3e-01	<0.001
CHD5	1.36465549	0.000340142	1.6	<0.001
CHD3	1.568155448	0.007182613	4.3	<0.001
CERS1	1.256482733	0.006187944	2.5e-01	<0.001
CELF4	1.266315192	0.000502411	3.2	<0.001
CEACAM6	0.830447969	0.006481502	4.4	<0.001
CDS1	0.619434738	0.00328904	3.2e-01	<0.001
CDHR2	0.847514909	0.003798721	2.9	<0.001
CDH17	0.729770539	0.000635009	1.4e-01	<0.001
CDC25C	0.684151197	0.00688226	8.2	<0.001
CCRL2	0.677114592	0.002178477	5.3e-01	<0.001
CCNA2	0.676285748	0.00597114	7.3e-04	<0.001
CAVIN1	1.354009446	0.004433824	2.7	<0.001
CATSPERG	1.370530111	0.007056119	3	<0.001
CARNS1	1.264766074	0.00669264	1.5	<0.001
CADPS	0.867620712	0.008019302	1.8	<0.001
C7	1.154533485	0.000912349	11	<0.001
C4orf50	1.306276285	0.009847324	2.2	<0.001
C1QL4	1.265743223	0.006675407	3.9e-01	<0.001
C19orf81	1.223741881	0.004326188	5.9e-01	<0.001
C16orf96	1.331680254	0.005459506	3.9e-01	<0.001
BST2	1.245735057	0.002990982	4.0e-01	<0.001
BHMG1	1.326825141	0.000415561	7.0e-01	<0.001
AXIN2	0.814861386	0.003939369	2.6e-01	<0.001
ATP6V1B1	1.397896547	1.29412E-05	1.5e-01	<0.001
ATP2A1	1.364043136	0.001518394	15	<0.001
ASPG	0.828092956	0.002850215	4.1e-01	<0.001
ARV1	0.645960387	0.006296874	160	<0.001
ARHGEF17	1.47498475	0.00307932	5	<0.001
APELA	0.81227505	0.006766816	5.2e-01	<0.001
APC2	1.595680863	0.00064022	61	<0.001
AOC2	1.319226342	0.003690611	1.9e-01	<0.001

Indexed in: [Current Contents/Clinical Medicine] [SCI Expanded] [ISI Alerting System] [ISI Journals Master List] [Index Medicus/MEDLINE] [EMBASE/Excerpta Medica] [Chemical Abstracts/CAS]

Gene symbol	Univariate analysis		Multivariate analysis	
	HR	P-value	HR	P-value
ANKS4B	0.657463731	0.000561344	6.7e-02	<0.001
ANKRD22	0.730856239	0.002877536	2.1	<0.001
ANAPC5	0.4607465	0.0094694	7.8e-03	<0.001
AIF1L	1.281527978	0.003975246	14	<0.001
AGMAT	0.701313746	0.009415433	10	<0.001
AGFG1	0.471524071	0.008488669	9.8e-04	<0.001
ADARB1	1.742317631	0.000124682	1.3e-01	<0.001
ADAM9	0.686991601	0.00312403	100	<0.001
ADAM11	1.388217427	0.000336073	3.8e-01	<0.001
ACOT11	0.679141782	0.004708273	9.4	<0.001
AC129492.1	1.368845979	0.002649713	4.9e-02	<0.001
AC009336.2	1.302764599	0.000840112	5.8e-01	<0.001
CD1A	0.761654995	0.000272979	7.2e-01	0.001
STARD9	1.264169741	0.008620268	1.4	0.002
DAPK1	1.249692788	0.008324465	1.3	0.002
DSG4	0.782143447	0.002206743	1.3	0.003
TMEM88	1.561816138	0.000335998	6.6e-01	0.005
FAM151B	0.623891263	0.00218039	6.1e-01	0.005
SYCE2	1.308137768	0.009435619	7.1e-01	0.007
JPH3	1.233591685	0.004498381	8.0e-01	0.008
JDP2	1.704624037	0.00979684	5.3e-01	0.011
ZDHHC3	0.40145391	0.000119984	2.2	0.015
CCL24	0.857409516	0.005718276	8.5e-01	0.015
ALDOB	0.884387033	0.009297044	1.1	0.019
RIMKLB	1.264805716	0.009187316	7.6e-01	0.022
C10orf55	0.753029457	0.008084309	1.3	0.023
F2RL2	0.82236627	0.00801046	8.3e-01	0.042
ANXA3	0.767488008	0.002450007	8.0e-01	0.045
ALPP	1.143185335	0.007108907	1.1	0.045

References:

1. Jemal A, Bray F, Center MM et al: Global cancer statistics. Cancer J Clin, 2011; 61(2): 69–90
2. Chen W, Zheng R, Baade PD et al: Cancer statistics in China, 2015. Cancer J Clin, 2016; 66(2): 115–32
3. Zhang B, Pan X, Cobb GP, Anderson TA: microRNAs as oncogenes and tumor suppressors. Dev Biol, 2007; 302(1): 1–12
4. Tutar Y: miRNA and cancer; Computational and experimental approaches. Curr Pharm Biotechnol, 2014; 15(5): 429
5. Chou CH, Shrestha S, Yang CD et al: miRTarBase update 2018: A resource for experimentally validated microRNA-target interactions. Nucleic Acids Res, 2017; 46(D1): D296–302
6. Wong N, Wang X: miRDB: An online resource for microRNA target prediction and functional annotations. Nucleic Acids Res, 2015; 43(Database issue): D146–52
7. Yu G, Wang L-G, Han Y, He Q-Y: clusterProfiler: An R package for comparing biological themes among gene clusters. OMICS, 2012; 16(5): 284–87
8. Jian-Hua Y, Jun-Hao L, Peng S et al: starBase: A database for exploring microRNA-mRNA interaction maps from Argonaute CLIP-Seq and Degradome-Seq data. Nucleic Acids Res, 2011; 39(Database issue): D202–9
9. Volinia S, Calin GA, Liu CG et al: A microRNA expression signature of human solid tumors defines cancer gene targets. Proc Natl Acad Sci USA, 2006; 103(7): 2257–61

Indexed in: [Current Contents/Clinical Medicine] [SCI Expanded] [ISI Alerting System] [ISI Journals Master List] [Index Medicus/MEDLINE] [EMBASE/Excerpta Medica] [Chemical Abstracts/CAS]

10. Yan H, Wu J, Liu W et al: MicroRNA-20a overexpression inhibited proliferation and metastasis of pancreatic carcinoma cells. Hum Gene Ther, 2010; 21(12): 1723–34
11. Xiong Y, Zhang L, Kebebew E: MiR-20a is upregulated in anaplastic thyroid cancer and targets LIMK1. PLoS One, 2014; 9(5): e96103
12. Sanfiorenzo C, Ilie MI, Belaid A et al: Two panels of plasma microRNAs as non-invasive biomarkers for prediction of recurrence in resectable NSCLC. PLoS One, 2013; 8(1): e54596
13. Qiang XF, Zhang ZW, Liu Q et al: miR-20a promotes prostate cancer invasion and migration through targeting ABL2. J Cell Biochem, 2014; 115(7): 1269–76
14. Ogawa R, Ishiguro H, Kuwabara Y et al: Expression profiling of micro-RNAs in human esophageal squamous cell carcinoma using RT-PCR. Med Mol Morphol, 2009; 42(2): 102–9
15. Malzkorn B, Wolter M, Liesenberg F et al: Identification and functional characterization of microRNAs involved in the malignant progression of gliomas. Brain Pathol, 2010; 20(3): 539–50
16. Schetter AJ, Leung SY, Sohn JJ et al: MicroRNA expression profiles associated with prognosis and therapeutic outcome in colon adenocarcinoma. JAMA, 2008; 299(4): 425–36
17. Yu Z, Willmarth NE, Zhou J et al: microRNA 17/20 inhibits cellular invasion and tumor metastasis in breast cancer by heterotypic signaling. Proc Natl Acad Sci USA, 2010; 107(18): 8231–26
18. Fan X, Liu Y, Jiang J et al: miR-20a promotes proliferation and invasion by targeting APP in human ovarian cancer cells. Acta Biochim Biophys Sin (Shanghai), 2010; 42(5): 318–24
19. Kang HW, Wang F, Wei Q et al: miR-20a promotes migration and invasion by regulating TNKS2 in human cervical cancer cells. FEBS Lett, 2012; 586(6): 897–904
20. Huang G, Nishimoto K, Zhou Z et al: miR-20a encoded by the miR-17-92 cluster increases the metastatic potential of osteosarcoma cells by regulating Fas expression. Cancer Res, 2012; 72(4): 908–16
21. Lin S, Gregory RI: MicroRNA biogenesis pathways in cancer. Nat Rev Cancer, 2015; 15(6): 321–33
22. Hansen IA, Sieglaff DH, Munro JB et al: Forkhead transcription factors regulate mosquito reproduction. Insect Biochem Mol Biol, 2007; 37(9): 985–97
23. Zhang W, Duan N, Song T et al: The emerging roles of Forkhead Box (FOX) proteins in osteosarcoma. J Cancer, 2017; 8(9): 1619–28
24. Perez-Sanchez C, Gomez-Ferreria MA, de La Fuente CA et al: FHX, a novel fork head factor with a dual DNA binding specificity. J Biol Chem, 2000; 275(17): 12909–16
25. Perez-Sanchez C, Arias-de-la-Fuente C, Gomez-Ferreria MA et al: FHX.L and FHX.S, two isoforms of the human fork-head factor FHX (FOXJ2) with differential activity. J Mol Biol, 2000; 301(4): 795–806
26. Choi VM, Harland RM, Khokha MK: Developmental expression of FoxJ1.2, FoxJ2, and FoxQ1 in *Xenopus tropicalis*. Gene Expr Patterns, 2006; 6(5): 443–47
27. Wijchers PJ, Hoekman MF, Burbach JP, Smidt MP: Identification of forkhead transcription factors in cortical and dopaminergic areas of the adult murine brain. Brain Res, 2006; 1068(1): 23–33
28. Kehn K, Berro R, Alhaj A et al: Functional consequences of cyclin D1/BRCA1 interaction in breast cancer cells. Oncogene, 2007; 26(35): 5060–69
29. Wang Y, Yang S, Ni Q et al: Overexpression of forkhead box J2 can decrease the migration of breast cancer cells. J Cell Biochem, 2012; 113(8): 2729–37
30. Chen X, Cao X, Tao G et al: FOXJ2 expression in rat spinal cord after injury and its role in inflammation. J Mol Neurosci, 2012; 47(1): 158–65
31. Qiu X, Ji B, Yang L et al: The role of FoxJ2 in the migration of human glioma cells. Pathol Res Pract, 2015; 211(5): 389–97
32. Yang Q, Cao X, Tao G et al: Effects of FOXJ2 on TGF-beta1-induced epithelial-mesenchymal transition through Notch signaling pathway in non-small lung cancer. Cell Biol Int, 2017; 41(1): 79–83

Indexed in: [Current Contents/Clinical Medicine] [SCI Expanded] [ISI Alerting System] [ISI Journals Master List] [Index Medicus/MEDLINE] [EMBASE/Excerpta Medica] [Chemical Abstracts/CAS]